Experimental investigation of joint with positive eccentricity in CFS truss

Małgorzata Gordziej-Zagórowska [a], Elżbieta Urbańska-Galewska [a], Patryk Deniziak [a]
[a] *Department of Civil and Environmental Engineering, Gdańsk University of Technology, Poland*

1

Abstract

2 Due to technological restrictions, in the case of trusses made of CFS open cross-sections,

3 positive eccentricities in the truss joints have become very frequent. Therefore studies

4 concerning the load-bearing capacity of truss joints with positive eccentricity were

5 undertaken. It was assumed that the resistance of cold-formed steel (CFS) open cross-

6 section truss joints located on compression chords and with positive eccentricity is greater

7 than that which results from hitherto known methods of steel structure dimensioning. In order

8 to confirm the hypothesis, experimental studies were conducted. A series of 5 full-scale

9 research models was subjected to destructive tests to determine the deformation forms and

10 strains of the hat-section walls in the area of the eccentric joint. Forms of truss chord stability

11 loss under compression and bending were identified.The course of research and analysis of

12 results were described in the article. Than comparative analysis of the outcomes of the

13 experimental tests and the results of analytical calculations carried out according to

14 Eurocode standards was done, and the obtained results confirmed the usefulness of the

15 undertaken research. The obtained results did not allow for explicit confirmation of the

16 research hypothesis at this stage, but constituted the basis for validation of the numerical

17 model which has been elaborated. Currently, the authors carry out a variety of numerical

18 analysis.

1. Introduction

20 Cold-formed steel (CFS) members are used more and more commonly in industrial

21 buildings, not only as secondary framing members but also as main bearing elements such

22   as roof trusses and columns. As a result, new research problems appear. Both individual

23   structural elements such as beams and columns [1–4] and entire parts of the structure,

24   including lattice girders, are subjected to testing [5–7].

25   Modern lightweight technology used in the production of steel trusses affects their

26   shape, particularly the construction of joints and, as a result, eccentricities frequently appear

27   in the trusses' joints. This can induce additional local bending and shearing forces in the

28   truss chords [8]. In the case of lattice structures composed of circular, square or rectangular

29   hollow sections, the eccentricity influence on the static design resistances of the welded

30   joints has been precisely investigated [9,10]. Detailed information about such joints can be

31   found, among others in publications [9], [11], [12], [13] and in the standard [14]. The

32   information included in these works shows that the load carrying capacity of joints with

33   positive eccentricities is lower than that of joints without eccentricities (e=0). On the other

34   hand, in joints with negative eccentricities the opposite is true; their load carrying capacity is

35   higher.

36   However, in the case of trusses made of CFS open cross-sections, diagonals are

37   attached to chords by bolts. Trusses' chords are most often designed with hat-sections or

38   members made of two channels, and diagonals are usually made of single channel sections.

39   The use of the above mentioned open cross-sections affects the way joints are shaped.

40   Diagonals are inserted into the cross-sections of the chords, as was done in [6,15], or as

41   presented in Figure 1. The proper arrangement of mechanical connectors in the truss joints

42   causes that brace members must be shifted outside, as shown in Figure 1. This results in the

43   creation of positive eccentricities in the truss joints, and hence bending moments and shear

44   forces in the chords of lattice girders. Those additional internal forces should be taken into

45   account when truss members are designed.

46   In engineering practice, the dimensioning of truss chords made of CFS members

47   taking into account positive eccentrics, in accordance with current European standards

48   [14,16–18], is performed using a simplified method. However, taking into account the

49   additional bending and shear between the points of intersection of the diagonals' axes

2

50 causes an increase in the strain of the bottom chord cross-section in the area of the joint. As

51 a result, the cross-section of the chord should be increased along its entire length or, as

52 presented in the work [19], strengthening cover plates should be made in the nodal zone

53 (Fig.2).
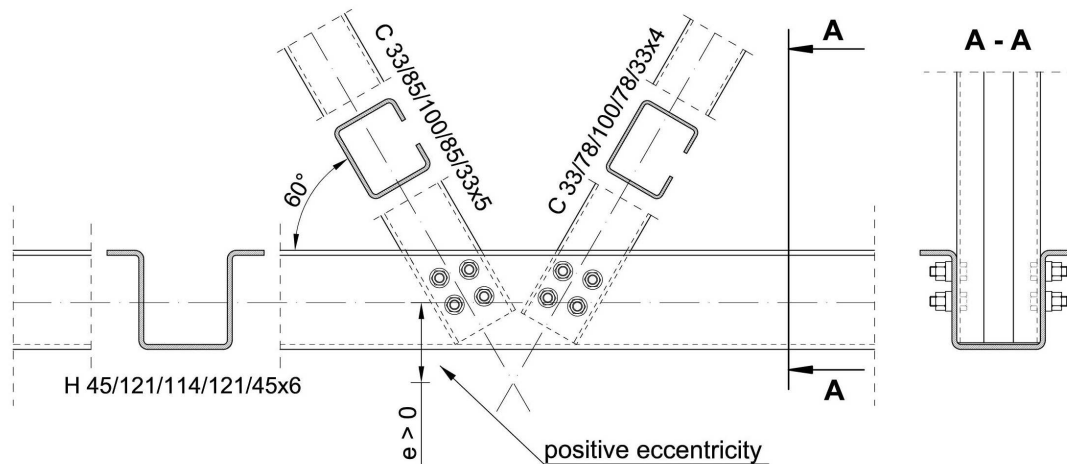
54

55 **Fig.1.** Positive eccentricity in the bolted truss joint made from CFS open cross-sections.
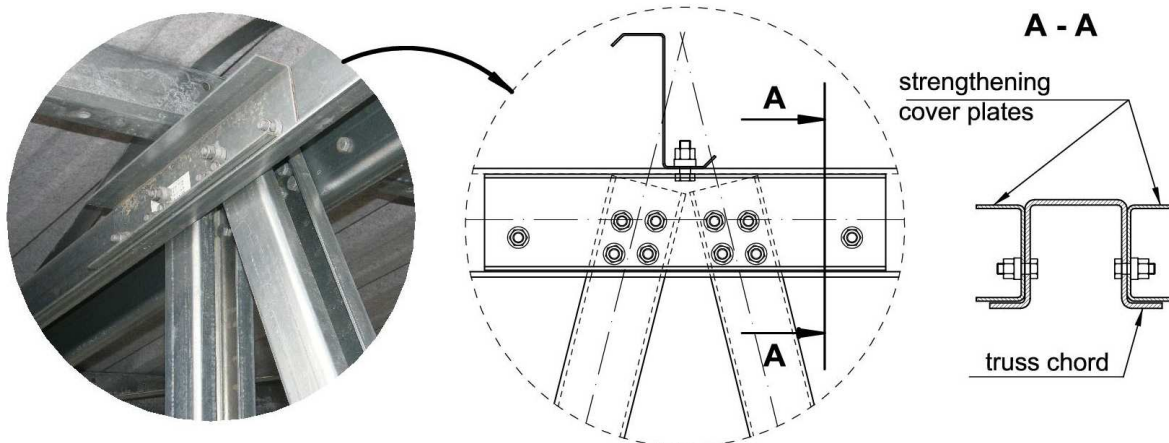
56

57 **Fig.2.** Joint with strengthening cover plates [8].

58 **2. State of the art**

59   Most of the studies of CFS members undertaken so far have been carried out on

60 single compressed [20–23] or bent structural elements [3,24–28]. The issue of wall stability

61 under the influence of shear and bending was investigated by Pham and Hancock [29,30],

62 and the results of experimental studies were used to validate the FEM model. Crisan,

3

63   Ungureanu, and Dubina, in turn, conducted full-scale stability tests of both perforated

64   sections [31] and high storage racks composed of these [32].

65   Particularly noteworthy are the tests carried out on complex structural elements such

66   as truss girders. Jankowska-Sandberg and Kołodziej [5] carried out a full-scale examination

67   of the stability of trusses made out of hollow sections while Iwicki and Krajewski [33]

68   examined the stability of trusses on models in a 1:4 scale. The top and bottom chords of the

69   tested truss consisted of two angles and, additionally, battens were applied in the top chord,

70   while the diagonals were made from closed cross-sections. The above-mentioned studies

71   concerned the stability of the top and bottom truss chords at different transverse support

72   conditions of both chords.

73   In fact, few experiments concern studies of trusses made of CFS open cross-

74   sections. Dawe, Liu, and Li [7] conducted experimental research testing thirteen full-scale

75   triangular truss specimens made of cold-formed C-section with edge stiffeners. Connections

76   in the joints were made using self-drilling screws. Additionally, gusset plates were used in the

77   supporting and ridge joints. Specimens were fabricated in three pitches: 4:12, 6:12, and 8:12.

78   The aim of the experiments was to investigate the impact of the top chord inclination and the

79   effectiveness of various methods of strengthening the heel connection on the increase in the

80   load capacity of the truss. Analysis of the top chord inclination showed that an increase in

81   truss pitch resulted in an increase in the load capacity of truss specimens. For comparative

82   purposes, DSM (Direct Strength Method) analysis was also performed and calculations were

83   carried out using the recommendations of Canadian standards CSA.

84   Dizdar, Baran and Topkaya [34] conducted experimental and numerical tests on 17

85   full-scale floor trusses made of cold formed sigma-type cross-sections with edge stiffeners.

86   Diagonals were attached to chords by making use of rivets or self-tapping screws. Both the

87   rigidity and bearing load capacity of the trusses were tested depending on such parameters

88   as the wall thickness of the section, the number of connection fasteners used in the joint, and

89   the method of connecting the diagonals with the chords.

4

90   Reda et al. [35] performed experimental tests on 12 triangular roof trusses made of

91   CFS C-sections. Experimental studies allowed for a numerical model to show the actual

92   behavior of the structure. The aim of the study was to investigate the overall behavior of CFS

93   trusses using finite element analysis to predict the location of the truss failure and its cause

94   by calculating the demand to capacity (D/C) ratio using the Direct Strength Method (DSM) for

95   each component of the truss and comparing this with the results of FE analysis. The

96   presented procedure for calculating the D/C ratio can contribute to simplifying the

97   engineering design process by omitting the time-consuming FEM analysis.

98   In turn, Song et al. [36] performed tests on 5 trusses made of CFS sections joined by

99   means of a self-piercing riveted (SPR) connection. The trusses were subjected to point

100   bending. The influence of the trusses' height and span on their flexural stiffness and ultimate

101   bearing capacity was investigated. As a result of parametric analyses, a theoretical formula

102   was proposed to calculate the equivalent flexural stiffness of the trusses with SPR

103   connections. As the formula agreed with the experiment's results, it was concluded that the

104   proposed theoretical formula is valid and can be applied to practical engineering. Not only

105   was the flexural stiffness and load capacity the subject of the carried out research but also

106   lateral buckling of chords. Konkong et al. [37] studied the lateral buckling of a CFS cantilever

107   truss. The object of their interest was expressions for the buckling length factor which are

108   presented in AISI [38] and the Eurocode 3 [17] specification. Good conformity between

109   experimental and analytical results was stated. It had been shown that the values of the K-

110   factor by AISI and Eurocode 3 were too conservative for compression truss.

111   Zaharia and Dubina presented comprehensive studies on the rigidity of bolted joints

112   in truss joints made of CFS members in [39]. Experimental studies carried out over several

113   years were aimed at assessing the actual behavior of screw joints in trusses made of CFS

114   sections. Based on tests performed on single joints and on truss fragments, a theoretical

115   model of joint stiffness was proposed. The joint rigidity formula, which determines the

116   buckling length of the lattice members, was also checked by testing on a full-scale structure.

117   Much more experimental research on the joints and connections of the CFS truss

118   members was undertaken. Lim and Nethercot [40] investigated the stiffness of the shear

119   connection in the ridge joint of a portal frame made of CFS channel sections. The results of

120   experimental studies were compared with the results of the numerical analysis. The

121   dependence of the connection stiffness on the number of bolts and the bolt spacing in the

122   connection was proved. These studies were continued by Lim et al. [41]. Dubina [42]

123   described the full-scale tests of lap joints in portal frame joints made of CFS channel

124   sections.

125   Mathieson et al. [43,44] presented an innovative pin-joint connector called Howick

126   Rivet Connector (HRC). The research program began with experimental tests on T-joints.

127   Then, HRC connectors were proposed for the pinned joints in the trusses made of CFS

128   sections. Tests were carried out on a number of trusses made of chanel-section under static

129   and cyclic loading. Test results indicated that due to the shape of connectors considered,

130   they can have a positive effect on the joint stiffness.

131   Thus, eccentricities in the joints of modern truss structures made from CFS open

132   cross-sections are inevitable. However, the eccentricity influence on joint resistance has not

133   been studied so far. The knowledge on sectional instability modes local or distortional

134   buckling of individual plate elements at complex connections is still challenging and requires

135   more effort and attention from designers as they are not entirely covered by design code

136   procedures. Zaharina and Dubina [39] have already drawn attention to the need for such

137   research due to the lack of standard regulations in this area.

138   **3. Experimental investigation**

139   The currently used methods of shaping joints by introducing diagonals inside truss

140   chords (Fig. 1) cause that the joint area on the truss chord is stiffened by the walls of the

141   truss members. The support conditions in the part of the hat-section web in the area of the

142   analyzed truss chord joint are indicated in Figure 3.

143   Therefore, the following research hypothesis was assumed:

6

144 The resistance of truss joints made from CFS open cross-sections that are located on
145 compression chords and have positive eccentricity is greater than the resistance that results
146 from hitherto known methods of steel structure dimensioning. The increase in resistance in
147 the joint originates from the local support conditions of the plane elements of the hat-section
148 chord in the area of the truss joint.
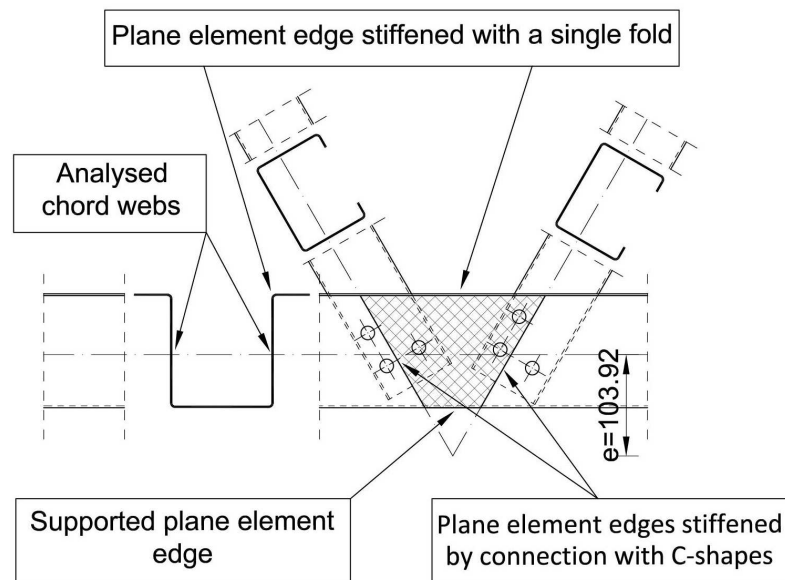
150 **Fig.3.** Support conditions of the hat-shaped section plane element in the area of the truss
151 joint.

152 In order to prove the above hypothesis, experimental studies of a typical joint used by one of
153 the well-known companies involved in the design and manufacturing of steel structures from
154 CFS sections were undertaken at Gdańsk University of Technology. Due to the high cost of
155 such studies, the experiment was carried out only for one wall thickness of sections, and the
156 obtained results allowed the development of a correct numerical model.

3.1. Experiment arrangement

3.1.1. Research model

159 Experimental studies were carried out in a laboratory of Gdańsk University of
160 Technology, Poland. A full-scale research model of the truss fragment made of CFS open
161 cross-sections was designed. The geometry of the truss adopted for testing is shown in

162 Figure 4a. Chords were made from the hat-section H 39/117/106/117/39x2, while diagonals

163 were made from the channel-section C 17/75/100/75/17x2 (Fig. 4b, c). Due to the shape of

164 the cross-sections used for the lattice member profiles (open cross-sections), the diagonals

165 were inserted into introduced inside the chords, as was done in [15], and [6]. With such a

166 method of joint shaping, screw connectors are most often used. In the investigated truss

167 segment, 6 bolts M12, class 8.8 were used in each joint (3 bolts on each web), as shown in

168 Figure 4a).

169 The joint with the value of the eccentricity e = 103.92 mm located on the compression chord

170 was tested, as only walls of compressed members are subjected to the local loss of stability.
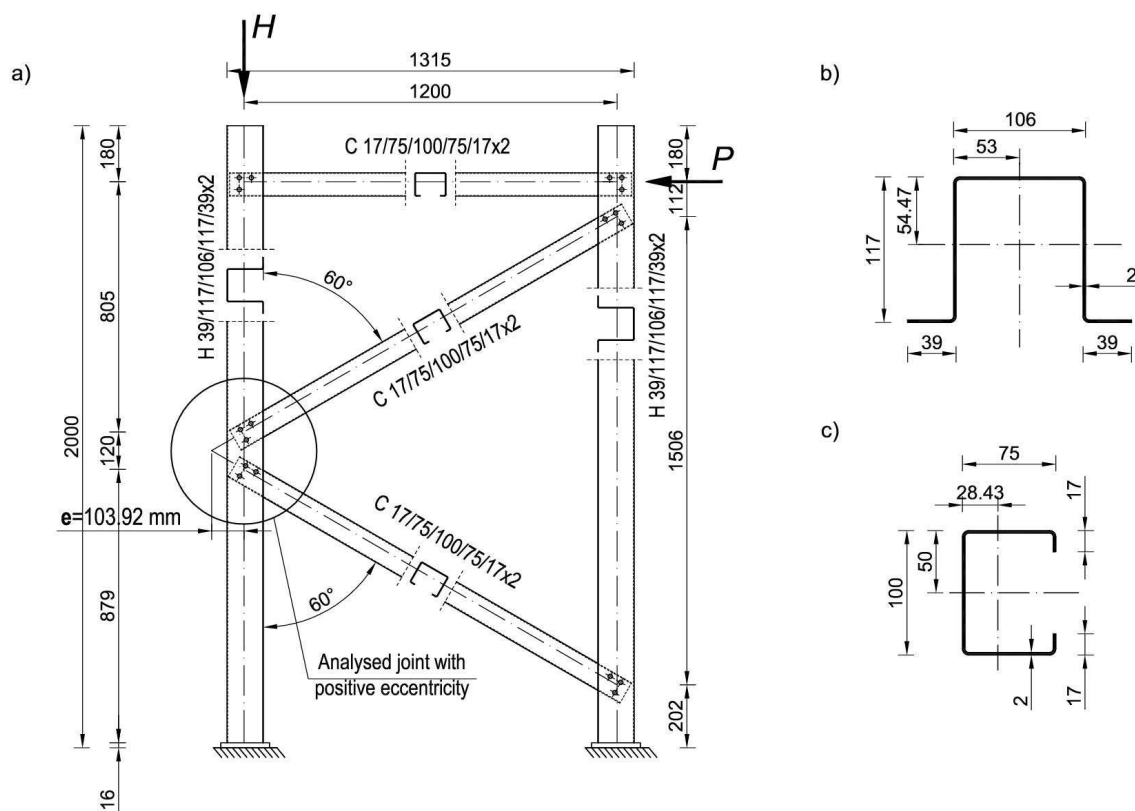
171

172 **Fig. 4.** a) research model; static scheme, dimensions of sections used in experimental tests

173 for: b) chords, c) diagonals. (All dimensions in mm)

174 **3.1.2. Research stage**

175 The static scheme of the research model is shown in Figure 4. The model was loaded

176 with two point forces H and P. Force H causes compression of the bottom chord, while force

8

177   P causes, due to the natural distribution of internal forces in the eccentric joint, local

178   shearing/bending of the bottom chord in the area of the joint. The use of a stationary actuator

179   to introduce force H (Fig. 5a) would change the static scheme of the cantilever mounted

180   tested model by immobilizing the free end of the truss in joint C. Therefore, a special

181   compression head was applied to introduce force H via two turnbuckles. This allowed for the

182   free displacement of joint C under the action of force P (Fig. 5b).
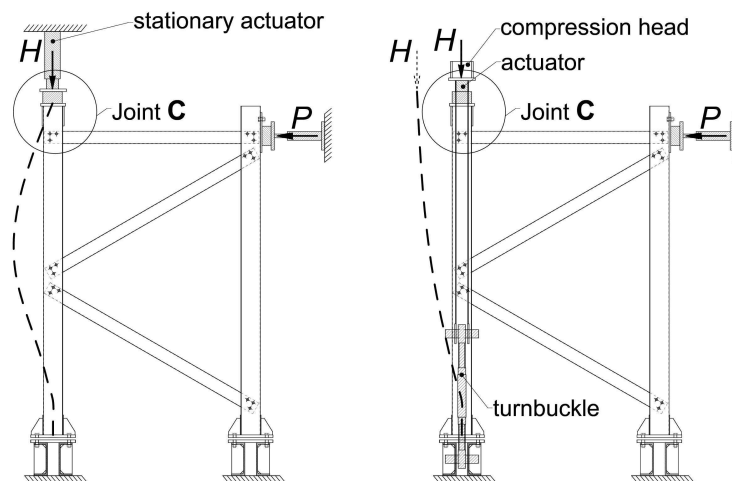
183

184   **Fig. 5**. Research model scheme of work when using: a) stationary actuator, b) compression

185   head [8].

186   One of the tested models fixed on the research station is shown in Figure 6. The stand was

187   developed after a series of preliminary numerical analyses and after the preliminary tests

188   described in [8,19]. The support and auxiliary elements of the experimental station were

189   painted yellow.

190
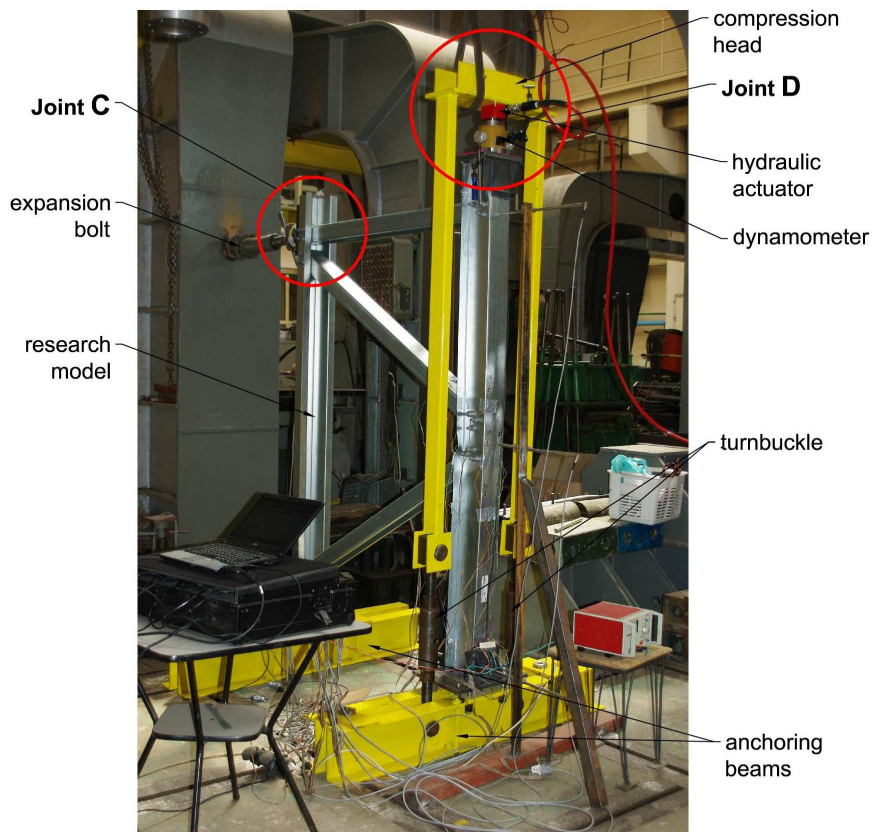
Fig. 6. Truss segment on the research station.

3.1.3. Applied instruments

The following measuring equipment was used during the tests. Seven inductive displacement sensors with a measuring range of ±100 mm were applied and arranged on the structure according to the diagram in Figure 7. The inductive sensors X and Y measured displacements of the research model in the bending plane, and sensor Z measured displacements out of the bending plane. Displacement sensors W1, W2, T1, and T2 were used to control possible horizontal and vertical displacements of support joints. For strain measurements, linear electrical resistance strain gauges LY11-6 / 120A were applied in four measuring cross-sections. The three cross-sections were placed on the compression chord (hat-section), respectively: 1-1 above the examined joint, 2-2 on the axis of the joint and 3-3 below the joint, and one additional cross-section 4-4 on the compression diagonal. The layout of the strain gauges in each of the cross-sections is shown in Figure 7. In total, 16 strain gauges were used, including one compensating strain gauge. Four strain gauges were

applied at every cross-section. Symmetrical about both local axes (z-z and y-y) strain gauges layout assured monitoring of the strains and type of stresses. The same values of the readings of the strain gauges A, B, C, and D indicated axial compression. In the case of bending about axis y-y, the readings were expected to be the same but only on two strain gauges at each side of the bending axis (A=C and B=D). When bending about axis z-z the equal readings were on the opposite sides of the bending axis (A=B and C=D).

During the tests, two point forces P and H were applied to the structure respectively by means of the expansion bolt and the actuator BVA HF2005 with a lifting capacity of 20 tons. The value of force P was registered using a dynamometer, N.B.C. Elettronica, with a nominal range of ±100 kN located between the expansion bolt that was causing force P and the tensioned chord of the structure, whereas the value of force H was measured by a CZAH CT 25 dynamometer with a rated load of 250 kN, located below the compression head and at the top of the compression chord of the research model.
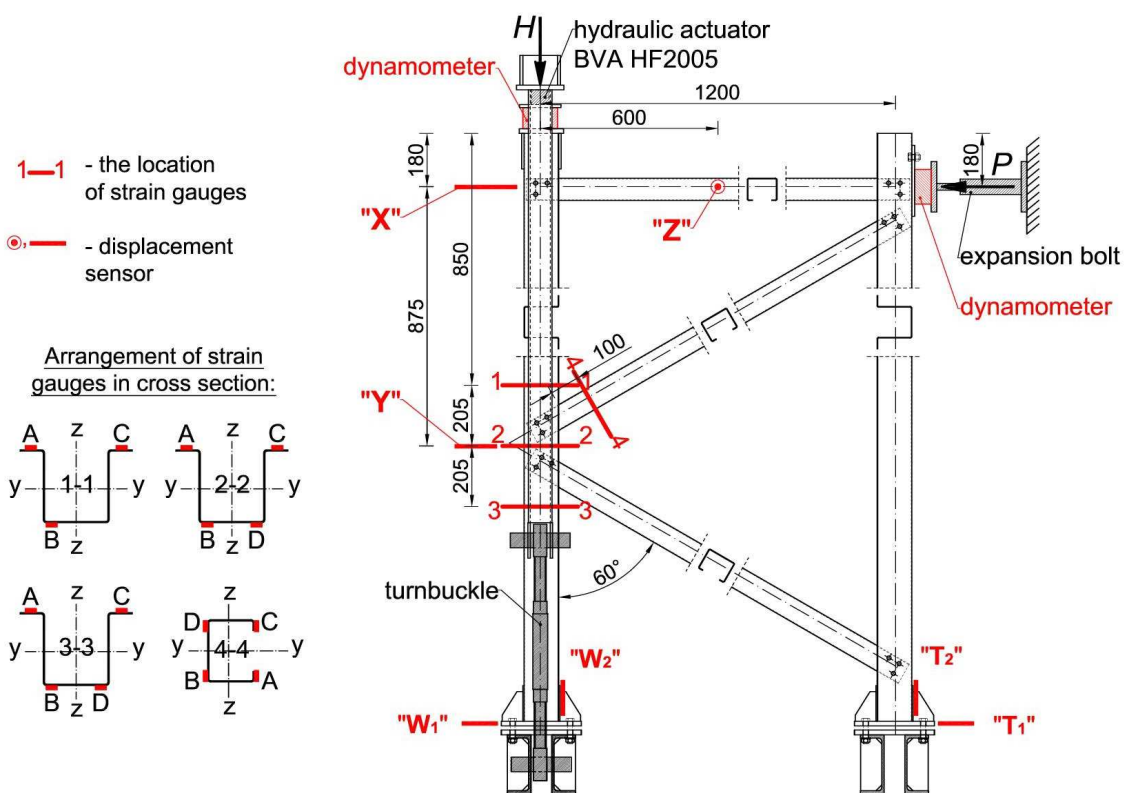
Fig. 7. Schematic layout of the measuring equipment on the research model.

3.2. The course and results of experimental studies

3.2.1. The course of experimental research

Five research models with subsequent numbers 1, 2, 3, 4 and 5 were subjected to testing. Procedures for preparing and conducting the described tests were carried out in accordance with the standard EN 1993-1-3 [17]. The destructive tests of the models were preceded by uniaxial tensile tests, which were the basis for identification of material constants and determination of the relation σ-ε of the steel material from which the members of research models were made. The tests were executed on samples cut from sections used for truss models build. 18 samples were gained from the hat section and 12 samples from the channel-section. Based on the obtained test results, the following average values of material properties were determined:

- hat-section E=210 GPa, f_y=398 MPa, f_u=489 MPa,
- channel-section E=199 GPa, f_y=366 MPa, f_u=445 MPa.

Load application to research models with turnbuckles was preceded by control and equalization of the tension force values in the tensioning elements of the compression head. Application of load to the structure was carried out at two stages:
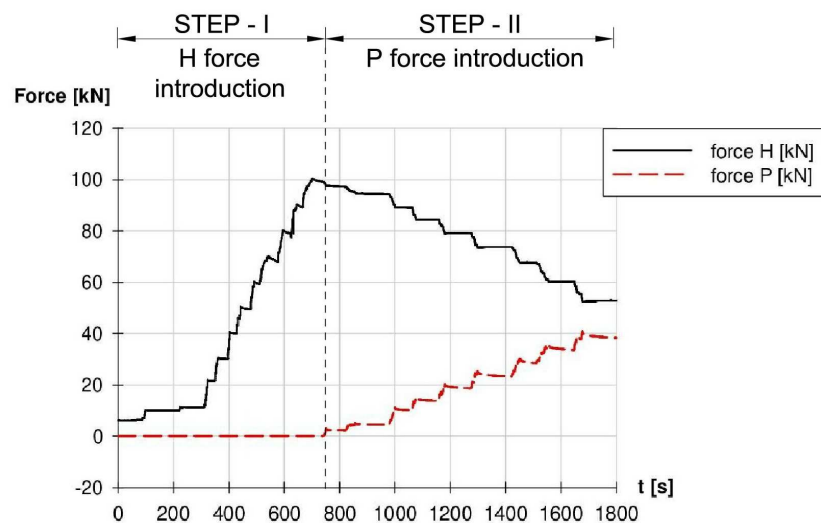
- Stage I - applying force H,
- Stage II - applying force P.

The forces were put on the structure by gradually increasing their value. Force H (compression) was introduced in 10 kN increments until the value of 100 kN was reached. From that moment, the value of force H was not changed as its task was only to achieve a certain level of normal stress in the analyzed cross-section. Next, the second stage of loading proceeded, i.e. the introduction of force P, with a step of 5 kN. There was a local loss of stability of member walls in the area of the analyzed joint (Fig. 11a) in all five models, already within the range of force P values from 5 kN to 10 kN. However, the bending load P was still increased up to a value of about 40 kN in order to determine the mechanisms of

12

246 destruction of the bending joint area (Fig. 11b). The course of introduced loads at time "t"

247 recorded during destructive tests is shown in Figure 8 as illustrated in the results obtained

248 during the testing of model No. 4. It should be noted that the time course of the load was

249 analogous in all five models.

250   Based on the analysis of the course of the introduced load, it can be seen that an

251 increase in the value of force P causes a simultaneous decrease in the value of force H (Fig.

252 8). It should be pointed out that after starting the introduction of load P, it was not possible to

253 maintain the value of force H at a constant level due to the instrumentation used. At the

254 same time, it should be noted that this fact was not significant due to the purpose of the

255 study, which was to lead to a possible destruction of the compression chord under the

256 influence of bending moment load in the area of the analyzed joint. However, the values of

257 both forces were accurately recorded (Fig. 8).

259 **Fig. 8.** Load history in time "t" registered during tests, as illustrated in based on the example

260 of model No. 4.

261 **3.2.2. Results of research**

262   Due to the purpose of the study, which was to determine the forms of deformation of

263 the hat-section walls and strains near the analyzed joint while applying the load, the strain

264 values were registered with strain gauges in four measuring cross-sections (Fig. 7). The

13

265 courses of strains as a function of time, specified in all four measurement cross-sections and

266 registered during tests on model No. 4 are shown in Fig.9.

267
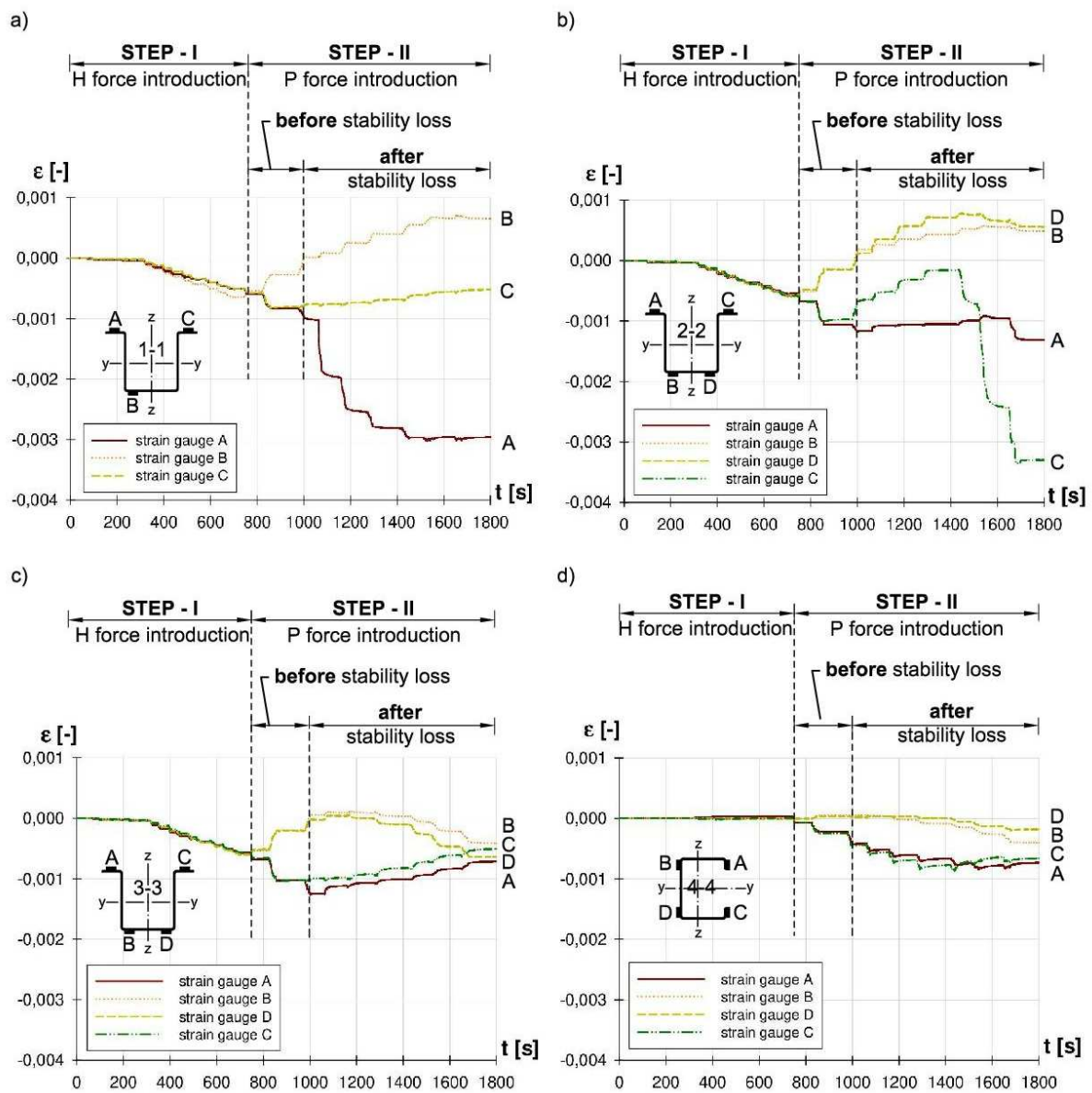
Fig. 9. The course of strains as a function of time in cross-sections: a) 1-1, b) 2-2, c) 3-3, d) 4-4, as illustrated in model No. 4 (description in the text).

270 Based on the charts presented in Figure 9, it was observed that at the first stage of the

271 loading, i.e. while introducing force H, there is compliance between the readings of the strain

272 gauges A, B, C and D in all four measuring cross-sections, which indicates an even

273 distribution of stress in the compressed cross-section. In addition, it should be pointed out

274 that at the first stage of loading no forms of deformations of the research model members

275 were observed. During the second stage of loading, in the range before local loss of stability,

276 symmetrical increases (A, C strain gauges) or reductions (B, D strain gauges) of cross-

277 sectional strains were observed relative to the local y-y axis ("clean" bending). Nevertheless,

278 in the range after the loss of stability, it was observed that the deformation shape loses its

279 symmetrical form. The cantilever walls of the hat-sections were characterized by different

280 directions of strains (measured with A and C strain gauges). The lack of symmetry relative to

281 the local z-z axis during deformation is caused by the existence of various imperfections.

282 Forms of truss chord stability loss under compression and bending identified on the

283 basis of the destructive tests of five research models are presented in Figure 10. The loss of

284 stability always started in the measuring cross-section 2-2 and, as the load increased,

285 deformations increased gradually. In all examined cases only a local form of loss of stability

286 occurred, what is visible in Figures 10, 11a and 11b. Typical plastic mechanism of failure

287 when columns build from open cross-sections are subjected to eccentric compression [45,46]

288 had been observed. It was CF1 when the flange is an outstanding compression element and

289 CW1 when the web of the cross-section is an internal compression element (flip disc type).
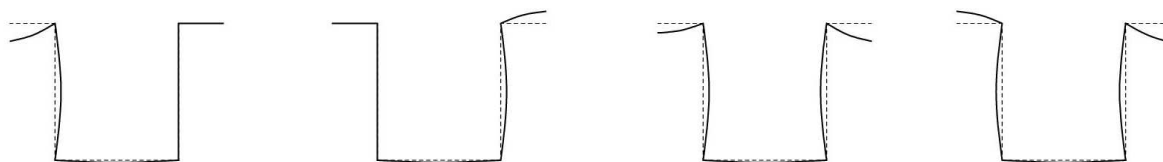
290

291 **Fig. 10.** Forms of truss chord local stability loss.

292 Deformation forms of the hat-section walls in the area of the analyzed joint at the

293 beginning of the stability loss are presented in Figure 11a, while Figure 11b presents the

294 deformation form of the hat-section observed during the experiment for the final stage of

295 loading (P=40 kN, H_{cor}=55 kN).

a) beginning of the
stability loss
(cross-section 2-2)

b) deformation
of the
hat-section
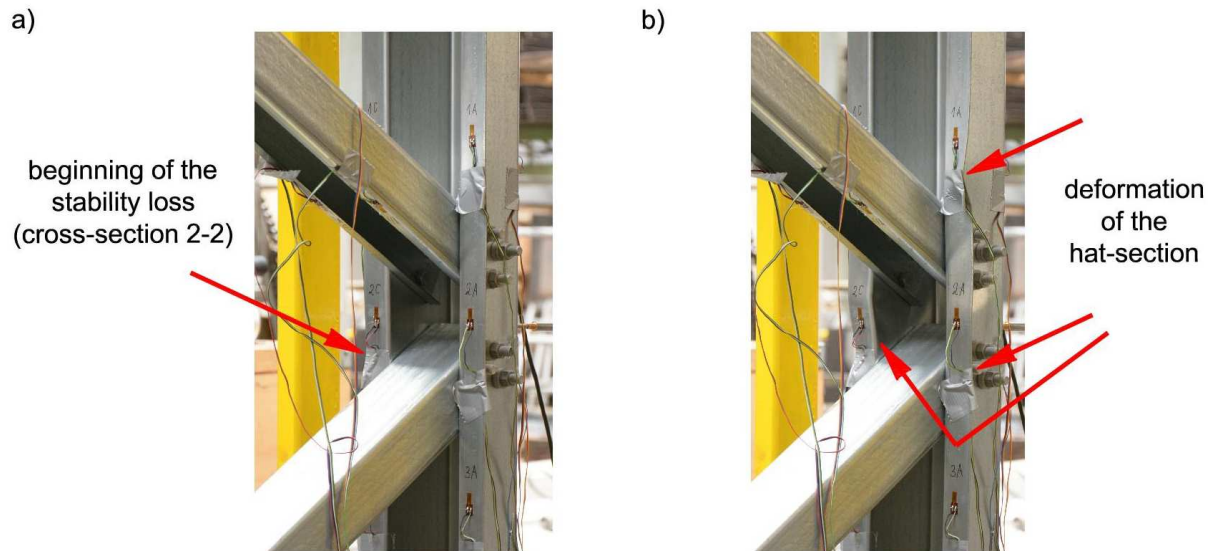
296

297 **Fig. 11.** a) beginning of the hat-section stability loss for the load value P=5 kN, H_{cor}=95 kN,

298 b) deformation of the hat-section chord at the final stage of the load.

299 The values of the external load of the research model as a set of forces, P and the

300 corresponding force H, are summarized in Table 1. These are the values at which the

301 beginning of the loss of local stability of the member walls in the vicinity of the analyzed joint

302 was observed. It was also observed that in all the research models in cross-section 2-2 or

303 directly in its vicinity, permanent deformations of the hat-section corners occurred. This

304 indicates that the material yield point was reached in this section area (Fig. 12). The yielding

305 state of the corners in the area of the analyzed joint was considered the limit state of the load

306 capacity of the analyzed cross-section.

plasticization of
hat-section corners

307
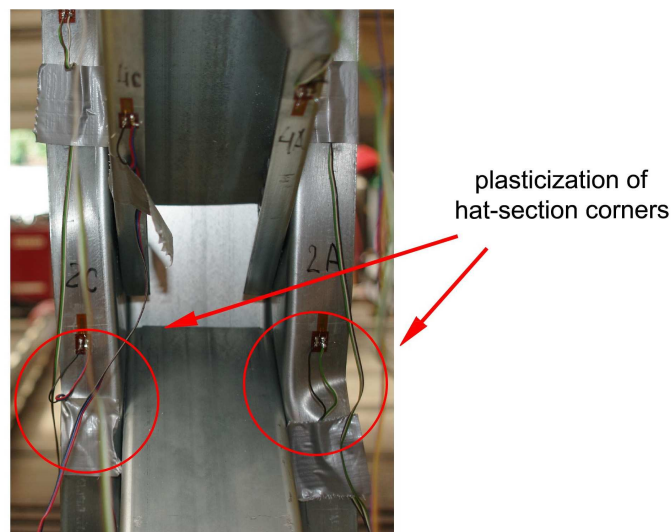
Fig. 12. Yielding of the hat-section corners in the measuring cross-section 2-2 (based on the example of research model no. 2).

Considering the above, the beginning of the stability loss observed during the tests can be qualified as the attainment of the critical state of the cross-section, and the load values given in Table 1 as the critical load of the research model (in the form of a set of P and H forces). When the above-mentioned load was reached, it was considered that the structure was working in a supercritical state until it reached the limit state. The observed variation of the forces P and H_{cor} is resulting from the "eye method" applied for identification of the stability loss moment during the conducted experiments. Received values of the forces were verificated with the use of elaborated diagrams presented in Figure 9. The variation of force P ranging from 5 to 8,5 KN is acceptable when statistical analysis is done. The test results presented in Table 1 showed good convergence of results for all models. All results are within +/- 2 standard deviations, which indicates good repeatability of the experiment.

Table 1. Listing of corresponding values of P and H_{cor} forces at which the local stability loss of the compressed chord of the truss model occurred.

Research model number	Force P [kN]	Average value of force P P_{av} [kN]	Standard deviation s_P [-]	Corresponding force H H_{cor} [kN]	Average value of force H $H_{cor,av}$ [kN]	Standard deviation s_H [-]
Model **1**	5.0			106		
Model **2**	8.5			96		
Model **3**	7.7	6.58	1.58	89	94.6	7.43
Model **4**	5.0			95		
Model **5**	6.7			87		

After carrying out destructive tests, the models were unscrewed to check for damage to fasteners and holes. It is visible in Figure 13 that there was no damage to the holes in the walls of the hat or channel-shaped sections. Bolts M12 class 8.8 used in the connection were also not damaged.

327
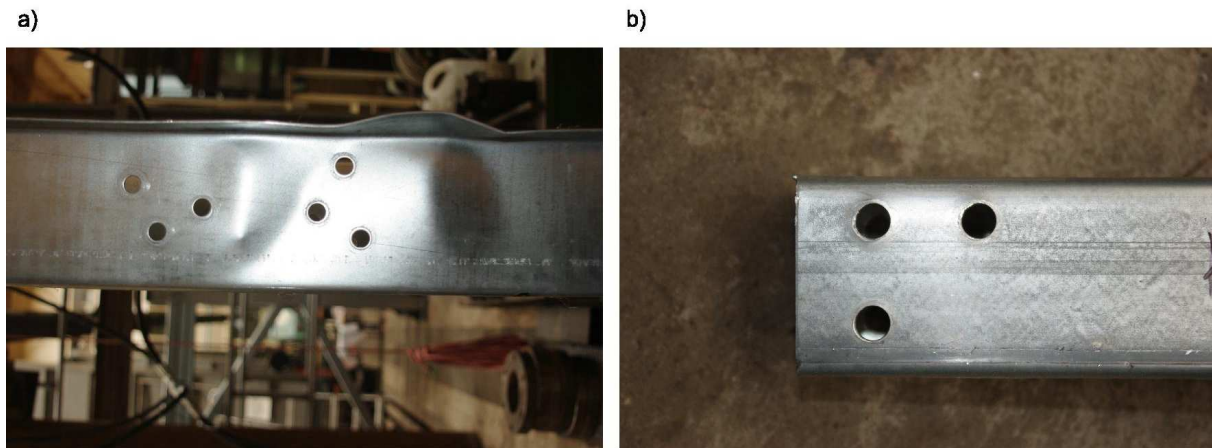
Fig. 13. View of bolt holes in deformed truss members during the experiment: a) hat-section,

b) channel-section.

Model displacements at X, Y and Z measurement points are shown in Figure 14. The lateral displacement values (in the plane perpendicular to the plane of the truss) resulting from the "Z" sensor and which ranged from -2.28 mm to 4.65 mm, were considered insignificant. In turn, the control of model support displacements showed minimal rotation and support displacement.

335
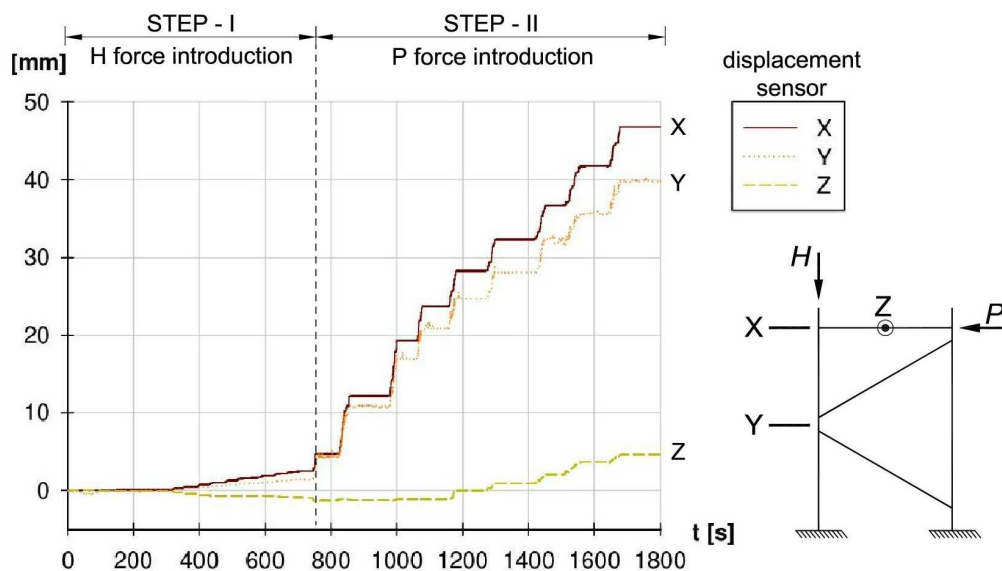
Fig. 14. Model displacements at X, Y, Z measurement points – illustrated in model No. 4.

4. Eurocode 3 design procedure.

338   For comparative purposes, the stress intensity of cross-sections 1-1, 2-2 and 3-3 in the

339   research truss joint was checked using analytical design procedures covered by European

340   standards [14,16–18].
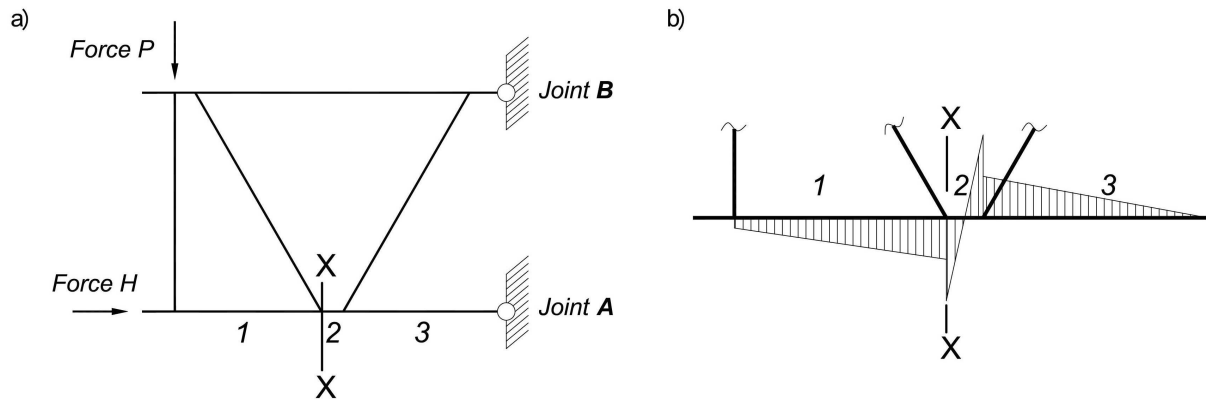
341

342   **Fig. 15.** a) Static scheme of the analyzed truss with the numbering of the compression chord

343   members, b) bending moment diagram at the compression truss chord.

344   In the analyzed case (Fig. 15), in the cross-section X-X (no 2), due to the positive

345   eccentricity that occurs, in addition to normal forces shear forces and bending moments also

346   occur. Taking into account the forces in member No 2 and in members No 1 and 3,

347   respectively, the effort of the cross-section was calculated on the basis of the standard

348   formula (1) [17]. The analysis was carried out in the elastic range. The calculations were

349   performed for an eccentricity with value e = 103.92 mm and sections with a wall thickness of

350   2 mm. The value of the eccentricity e = 103.92 mm results from the geometry of the truss

351   (angle of inclination of the diagonals), dimensions of the connected members, and the

352   connectors used.

353     $$N_{Ed}/N_{c,Rd}+(M_{y,Ed}+\Delta_{My,Ed})/M_{cy,Rd,com} \tag{1}$$

354   where:

355   N_{Ed} – design value of the compression force,

356     $M_{y,Ed}$ – design value of the bending moment (resulting from the eccentricity at the

357   joint),

358     $\Delta M_{y,Ed}$ – additional bending moment (due to a shift of the centroidal axis of the

359   effective cross-section relative to the centroidal axis of the gross cross-section

360   (for class 4),

361     $N_{c,Rd}$ – design resistance of a cross-section for uniform compression,

362     $M_{cy,Rd,com}$ – moment resistance for the maximum compressive stress in a cross-section

363   that is subjected only to moment about y-y axis.

364 It should be noted that, in accordance with the Eurocode procedure, for the calculations of

365 the degree of the cross-section effort to have value in engineering terms, the random nature

366 of both the loads and the research model should be taken into account. Loads in

367 experimental studies are deterministic. In order to obtain random values, 84% quantile of H

368 and P load values corresponding to mean values of H and P force increased by one standard

369 deviation respectively were used in calculations. Table 2 presents effort values in three

370 analysed cross-sections for four selected load cases (set of forces H and P).

371 **Table 2.** Effort of cross-sections of truss members Nos. 1, 2, 3 (according to Fig. 15)

e=103.92 mm					
quantiles of forces		Member no. / cross-section	Internal forces		Effort of the compression and bending cross-section [%]
H [kN]	P [kN]		N_{Ed} [kN]	M_{Ed} [kNm]	2.0 mm
108	0	1 (1-1)	107.79	0.13	70.58
		2 (2-2)	107.96	0	69.02
		3 (3-3)	108	0	69.05
102	6	1 (1-1)	101.94	0.38	70.05
		2 (2-2)	106.55	0.55	75.19
		3 (3-3)	111.10	0	71.03
85	23	1 (1-1)	85.35	1.24	70.50
		2 (2-2)	102.32	1.78	88.29
		3 (3-3)	119.88	0.39	81.65
57	47	1 (1-1)	57.95	2.56	69.94
		2 (2-2)	92.46	3.64	105.88
		3 (3-3)	128.28	0.77	91.91

372 When force P is equal zero, there is only axial compression and the effort of every one cross-

373 section was comparable. Introduction even a small value of the force P caused cross-section

374 bending due to the eccentric loading of the joint. This led to an increase in effort in the

375 measuring cross-section 2-2 in member 2 in comparison with the cross-sections 1-1 and 3-3

376 located on members 1 and 3. In summary, the introduction of force P resulted in the

377 following: The effort of the cross-section in member No. 2 (in the joint) is always greater than

378 the effort of the cross-section in members Nos. 1 and 3, which of course is associated with

379 the occurrence of shear forces and bending moments (a consequence of positive

380 eccentricity). At the final stage of the research model loading we are dealing with a special

381 case when the nodal cross-section is overloaded (as was confirmed by experimental tests)

382 while maintaining the resistance condition outside the joint. Therefore, it is logical that in a

383 design situation, exceeding the load capacity in the joint is already a signal for the designer

384 to increase the cross-section of the entire truss chord or make reinforcing cover plates (Fig.

385 2). So, according to the Eurocode procedure, the cross-sectional load capacity of the

386 eccentric joint is decisive when the truss chord cross-section is selected.

387 **5. Summary and conclusions**

388   The conducted experimental tests were aimed at obtaining information on the

389 behaviour of trusses made of CFS with positive eccentricity at joints, as well as obtaining the

390 research results in the form of a register of strains and displacements of both the model and

391 the joint. The calculations of the analyzed truss segment carried out in accordance with

392 Eurocode procedures coincide with the results of experimental tests for a truss made of 2

393 mm thick sections. Based on the experimental research the following conclusions were

394 made:

395 • Local buckling of the hat-section chord was observed.

396 • The loss of stability in all research models started in the middle of the joint, in the

397   vicinity of the measuring cross-section 2-2.

398 • Plastic mechanisms of failure occurred only in truss members.

399 • Neither bolts nor holes for fasteners were destroyed.

400 Due to the high cost of experimental research, destructive tests were limitated to one

401 wall thickness, so it was not possible to explicitly confirm the research hypothesis formulated

402 at this stage of work. In order to be able to answer the hypothesis, numerical analyses are

403 planned for the wall thicknesses: 1.0 mm, 1.5 mm, and 4.0 mm and for different eccentric

404 values. What is more the results of experimental tests will constitute the basis for validation

405 of the numerical models.

406 **6. References**

407 [1]   P. Deniziak, K. Winkelmann, TS-based RSM-aided design of cold-formed steel

408 stiffened C-sectional columns susceptible to buckling, Shell Struct. Theory Apl. (2018) 533–

409 536.

410 [2]   A. Crisan, V. Ungureanu, D. Dubina, Behaviour of cold-formed steel perforated

411 sections in compression: Part 2—numerical investigations and design considerations, Thin-

412 Walled Struct. 61 (2012) 97–105. https://doi.org/10.1016/j.tws.2012.07.013.

413 [3]   D. Dubina, V. Ungureanu, Behaviour of multi-span cold-formed Z-purlins with bolted

414 lapped   connections,   Thin-Walled   Struct.   48   (2010)   866–871.

415 https://doi.org/10.1016/j.tws.2010.04.003.

416 [4]   P. Paczos, K. Magnucki, Local buckiling of cold-formed thin-walled cannel beams with

417 drop flange, Adv. Trends Struct. Mech. Comput. - Zingoni Ed. (2010).

418 [5]   J. Jankowska-Sandberg, J. Kołodziej, Experimental study of steel truss lateral–

419 torsional   buckling,   Eng.   Struct.   46   (2013)   165–172.

420 https://doi.org/10.1016/j.engstruct.2012.07.033.

421 [6]   D. Visy, S. Adany, A.L. Joo, Finite element studies on the global buckling of cold-

422 formed trusses., Eighth Int. Conf. Adv. Steel Struct. (2015) 1–18.

423 [7]   J.L. Dawe, Y. Liu, J.Y. Li, Strength and behaviour of cold-formed steel offset trusses,

424 J. Constr. Steel Res. 66 (2010) 556–565. https://doi.org/10.1016/j.jcsr.2009.10.015.

425 [8]   M. Gordziej-Zagórowska, E. Urbańska-Galewska, P. Deniziak, Ł. Pyrzowski, Truss

426 joint with positive eccentricities – experimental research, Civ. Environ. Eng. Rep. (2017)

427 107–123.

428 [9]   J. Bródka, M. Broniewicz, Konstrukcje stalowe z rur, Arkady, Warszawa, 2001.

429 [10]   J. Bródka, M. Broniewicz, Konstrukcje stalowe z kształtowników zamkniętych, Polskie

430 Wydawnictwo Techniczne, Rzeszów, 2016.

431 [11]   J.A. Packer, J. Wardenier, Y. Kurobane, D. Dutta, N. Yeomans, Design guide for

432 rectangular hollow (RHS) joints under predominantly static loading., CIDECT Construction

433 with hollow stell sections, Koln, 1992.

434 [12]   J. Wardenier, Y. Kurobane, J.A. Packer, D. Dutta, N. Yeomans, Design guide for

435 circular hollow section (CHS) joints under predominantly static loading., CIDECT

436 Construction with hollow stell sections, Koln, 1991.

437 [13]   Y. Chen, J. Yang, K. Hu, Parametric study and formulae of SCFs for positive large

438 eccentricity CHS N-joints, J. Constr. Steel Res. 120 (2016) 117–131.

439 https://doi.org/10.1016/j.jcsr.2016.01.005.

440 [14]   EN 1993-1-8, Eurocode 3: Design of steel structures - Part 1-8: Design of joints, Eur.

441 Comm. Stand. (2005).

442 [15]   C. Basaglia, D. Camotim, GBT-based buckling analysis of cold-formed steel trusses,

443 Proc. Sixth Int. Conf. Thin Walled Struct. Timisoara Rom. (2011) 149–156.

444 [16]   EN 1993-1-1, Eurocode 3: Design of steel structures - Part 1-1: General rules and

445 rules for buildings, Eur. Comm. Stand. (2005).

446 [17]   EN 1993-1-3, Eurocode 3: Design of steel structures - Part 1-3: General rules -

447 Supplementary rules for cold-formed members and sheeting, Eur. Comm. Stand. (2006).

448 [18]   EN 1993-1-5, Eurocode 3: Design of steel structures - Part 1-5: General rules - Plated

449 structural elements, Eur. Comm. Stand. (2006).

450 [19]   M. Gordziej-Zagórowska, E. Urbańska-Galewska, Ł. Pyrzowski, P. Deniziak, A.

451 Łukowicz, Preliminary experimental research on stability of truss joint with positive

eccentricity., Recent Prog. Steel Compos. Struct. Proc. 13th Int. Conf. Met. Struct. Zielona Góra Pol. (2016) 425–432.

[20]   J. Ye, S.M. Mojtabaei, I. Hajirasouliha, Local-flexural interactive buckling of standard and optimised cold-formed steel columns, J. Constr. Steel Res. 144 (2018) 106–118. https://doi.org/10.1016/j.jcsr.2018.01.012.

[21]   J. Ye, I. Hajirasouliha, J. Becque, Experimental investigation of local-flexural interactive buckling of cold-formed steel channel columns, Thin-Walled Struct. 125 (2018) 245–258. https://doi.org/10.1016/j.tws.2018.01.020.

[22]   A. Łukowicz, E. Urbańska-Galewska, Deformations of innovative cold-formed GEB section., 7th Eur. Conf. Steel Compos. Struct. EUROSTEEL. (2014) 1–6.

[23]   M.S.H.M. Sani, F. Muftah, C.S. Tan, Experimental Analysis of Cold-Formed Steel C-Sections with the Notch Subjected to Axial Compression, KSCE J. Civ. Eng. 24 (2020) 1228–1239. https://doi.org/10.1007/s12205-020-2340-z.

[24]   M.R. Haidarali, D.A. Nethercot, Finite element modelling of cold-formed steel beams under local buckling or combined local/distortional buckling, Thin-Walled Struct. 49 (2011) 1554–1562. https://doi.org/10.1016/j.tws.2011.08.003.

[25]   D. Dubina, V. Ungureanu, L. Gîlia, Experimental investigations of cold-formed steel beams of corrugated web and built-up section for flanges, Thin-Walled Struct. 90 (2015) 159–170. https://doi.org/10.1016/j.tws.2015.01.018.

[26]   M. Kotełko, Load-capacity estimation and collapse analysis of thin-walled beams and columns—recent advances, Thin-Walled Struct. 42 (2004) 153–175. https://doi.org/10.1016/S0263-8231(03)00055-7.

[27]   C. Yu, B.W. Schafer, Simulation of cold-formed steel beams in local and distortional buckling with applications to the direct strength method, J. Constr. Steel Res. 63 (2007) 581–590. https://doi.org/10.1016/j.jcsr.2006.07.008.

[28]   A. Łukowicz, E. Urbańska-Galewska, M. Gordziej-Zagórowska, Experimental testing of innovative cold-formed GEB section., Civ. Environ. Eng. Rep. (2015) 129–140.

479 [29]   C.H. Pham, G.J. Hancock, Tension field action for cold-formed sections in shear, J.

480 Constr. Steel Res. 72 (2012) 168–178. https://doi.org/10.1016/j.jcsr.2011.12.001.

481 [30]   C.H. Pham, G.J. Hancock, Numerical investigation of longitudinally stiffened web

482 channels   predominantly   in   shear,   Thin-Walled   Struct.   86   (2015)   47–55.

483 https://doi.org/10.1016/j.tws.2014.09.005.

484 [31]   A. Crisan, V. Ungureanu, D. Dubina, Behaviour of cold-formed steel perforated

485 sections in compression. Part 1—Experimental investigations, Thin-Walled Struct. 61 (2012)

486 86–96. https://doi.org/10.1016/j.tws.2012.07.016.

487 [32]   A. Crisan, V. Ungureanu, D. Dubina, Influence of web members on the in-plane and

488 out-of-plane capacities of steel storage upright frames, Thin-Walled Struct. 81 (2014) 175–

489 184. https://doi.org/10.1016/j.tws.2013.10.024.

490 [33]   M. Krajewski, P. Iwicki, Stability and laod bearing capacity of a braced truss under

491 upward wind loading, Eurosteel. (2017).

492 [34]   C. Dizdar, E. Baran, C. Topkaya, Strength and stiffness of floor trusses fabricated

493 from   cold-formed   steel   lipped   channels,   Eng.   Struct.   181   (2019)   437–457.

494 https://doi.org/10.1016/j.engstruct.2018.12.041.

495 [35]   M. Reda, T. Sharaf, A. ElSabbagh, M. ElGhandour, Behavior and design for

496 component and system of cold-formed steel roof trusses, Thin-Walled Struct. 135 (2019) 21–

497 32. https://doi.org/10.1016/j.tws.2018.10.038.

498 [36]   L. Song, W. Yan, C. Yu, Z. Xie, Q. Tan, Flexural behavior investigation of the CFS

499 truss beams with self-piercing riveted connection, J. Constr. Steel Res. 156 (2019) 28–45.

500 https://doi.org/10.1016/j.jcsr.2019.01.014.

501 [37]   N. Konkong, T. Aramraks, K. Phuvoravan, Buckling length analysis for compression

502 chord in cold-formed steel cantilever truss, Int. J. Steel Struct. 17 (2017) 775–787.

503 https://doi.org/10.1007/s13296-017-6031-7.

504 [38]   AISI, North American specification for the design of cold-formed steel structural

505 members., Am. Iron Steel Inst. (2012).

[39] R. Zaharia, D. Dubina, Stiffness of joints in bolted connected cold-formed steel trusses, J. Constr. Steel Res. 62 (2006) 240–249. https://doi.org/10.1016/j.jcsr.2005.07.002.

[40] J.B.P. Lim, D.A. Nethercot, Stiffness prediction for bolted moment-connections between cold-formed steel members, J. Constr. Steel Res. 60 (2004) 85–107. https://doi.org/10.1016/S0143-974X(03)00105-6.

[41] J.B.P. Lim, G.J. Hancock, G. Charles Clifton, C.H. Pham, R. Das, DSM for ultimate strength of bolted moment-connections between cold-formed steel channel members, J. Constr. Steel Res. 117 (2016) 196–203. https://doi.org/10.1016/j.jcsr.2015.10.005.

[42] D. Dubina, Structural analysis and design assisted by testing of cold-formed steel structures, Thin-Walled Struct. 46 (2008) 741–764. https://doi.org/10.1016/j.tws.2008.01.030.

[43] C. Mathieson, K. Roy, G.C. Clifton, A. Ahmadi, J.B.P. Lim, Failure mechanism and bearing capacity of cold-formed steel trusses with HRC connectors, Eng. Struct. 201 (2019) 109741. https://doi.org/10.1016/j.engstruct.2019.109741.

[44] C. Mathieson, K. Roy, G.C. Clifton, A. Ahmadi, M. Rehan, J.B.P. Lim, Novel pin jointed moment connection for cold-formed steel trusses, Steel Compos. Struct. (2019) 453–467.

[45] V. Ungureanu, M. Kotełko, J. Grudziecki, Plastic mechanisms for thin-walled cold-formed steel members in eccentric compression, (2016).

[46] M. Kotełko, Nośność i mechanizmy zniszczenia konstrukcji cienkościennych., Wydawnictwo WNT, Warszawa, 2011.